New Phytologist

Research

Inferring climate from angiosperm leaf venation networks

Benjamin Blonder[1,2,3] **and Brian J. Enquist**[1,2,4]

[1]Department of Ecology and Evolutionary Biology, University of Arizona, PO Box 210088, Tucson, AZ 85721, USA; [2]Rocky Mountain Biological Laboratory, Gothic, CO 81224, USA; [3]Center for Macroecology, Evolution, and Climate, University of Copenhagen, 2100 Copenhagen, Denmark; [4]The Santa Fe Institute, Santa Fe, NM 87501, USA

Author for correspondence:
Benjamin Blonder
Tel: +1 520 626 3336
Email: bblonder@email.arizona.edu

Received: *28 November 2013*
Accepted: *22 February 2014*

New Phytologist (2014)
doi: 10.1111/nph.12780

Key words: functional trait, leaf hydraulics, leaf venation network, paleoclimate reconstruction, vein density.

Summary

- Leaf venation networks provide an integrative linkage between plant form, function and climate niche, because leaf water transport underlies variation in plant performance.
- Here, we develop theory based on leaf physiology that uses community-mean vein density to predict growing season temperature and atmospheric CO_2 concentration. The key assumption is that leaf water supply is matched to water demand in the local environment. We test model predictions using leaves from 17 temperate and tropical sites that span broad climatic gradients.
- We find quantitative agreement between predicted and observed climate values. We also highlight additional leaf traits that may improve predictions.
- Our study provides a novel approach for understanding the functional linkages between functional traits and climate that may improve the reconstruction of paleoclimate from fossil assemblages.

Introduction

Identifying the mechanisms underlying the distribution of species across broad climatic gradients remains a central question in ecology (Westoby & Wright, 2006). Species' traits determine performance, which then should influence fitness in a given environment (McGill *et al.*, 2006). This central assumption in trait-based ecology predicts that species with certain traits should be associated with specific environments in which the traits are adaptive. While this framework is conceptually simple, identifying these trait–environment linkages has remained elusive (Weiher *et al.*, 1999; Díaz *et al.*, 2004; Soudzilovskaia *et al.*, 2013). In plants, leaf hydraulic traits may often mediate these linkages, because water transport between a plant and its environment determines many aspects of structure and growth (Tyree & Ewers, 1991; Sack & Holbrook, 2006).

Here, we test the hypothesis that leaf venation networks provide a mechanistic link between plant physiological functioning and climate. Because allocation to the venation network results in a trade-off between transport (Brodribb *et al.*, 2007) and the cost of constructing a leaf (Sack & Scoffoni, 2013), different venation geometries should be adaptive in climates with differing hydraulic environments (Brodribb *et al.*, 2010; de Boer *et al.*, 2012). Some data support a linkage between climate and the density of minor veins (VD, length of minor veins per unit leaf area, units mm^{-1}). In observational studies, variation in VD has been linked to climate, including temperature, precipitation and moisture availability. Species from warmer and drier sites tend to have higher VD (Sack & Scoffoni, 2013), although sometimes contradictory or weak relationships are found (Dunbar-Co *et al.*, 2009; Blonder *et al.*, 2013; Jordan *et al.*, 2013). Additionally, in experimental manipulations over developmental timescales, VD changes with light availability (Tumanow, 1927; Carins Murphy *et al.*, 2012) and humidity (Lebedincev, 1927). In paleoecological studies, VD appears to have increased over evolutionary time (Boyce *et al.*, 2009), especially during the Late Cretaceous (Feild & Brodribb, 2013), possibly driven by falling atmospheric CO_2 concentrations (Brodribb *et al.*, 2009; Feild *et al.*, 2011; but see (Boyce & Zwieniecki, 2012). Similarly, VD appears to vary adaptively in response to climate within some clades (Carlquist, 1959; Jordan *et al.*, 2013).

Our primarily empirical understanding of the linkage between vein traits and climate has made it difficult to predict and isolate the relationship between each vein trait and each dimension of climate and to make predictions for climate based on community-scale distributions of venation network traits. For these reasons, vein traits have not yet been widely adopted as paleoclimate proxies or climate indicators (Manze, 1967; Uhl & Mosbrugger, 1999) despite recent interest (Sack & Scoffoni, 2013). Leaves do offer a potentially powerful way to reconstruct climate, with extant methods based on statistical correlations between leaf size and shape (Wolfe, 1993; Royer *et al.*, 2005). The physiological justification for such correlations has been limited (Royer & Wilf, 2006). There is a case for building more predictive theory. Recent physiological models have established quantitative linkages between VD and other leaf traits (Blonder *et al.*, 2011, 2013; Sack *et al.*, 2012) or between vein traits and atmospheric CO_2 concentrations (Brodribb & Feild, 2010; de Boer *et al.*,

© 2014 The Authors
New Phytologist © 2014 New Phytologist Trust

2012; Boyce & Zwieniecki, 2012). However, some of these models are controversial (Sack *et al.*, 2013; Blonder *et al.*, 2014) and others are not yet able to predict how other dimensions of climate, such as temperature and moisture availability, modulate this trait–climate linkage. Articulating the linkages between leaf traits and climate could provide a useful approach for predicting community composition and species' climate niches.

Here, we develop theory for how variation in climate selects for communities with species with certain venation network geometries. By extending extant physiological models, we provide equations that couple variation in leaf physiology to variation in ambient temperature and atmospheric concentrations of CO_2. Our central hypothesis is that the maximum rate of water supply to the leaf (transpiration rate; E) is coupled to the maximum potential water demand of the environment (potential evapotranspiration; PET) as $E = \alpha$ PET, where α is a dimensionless coefficient reflecting potential differences in plant water-use efficiency and site hydrology. The model defines E, α and PET in terms of minor vein density (VD), growing season temperature (T_c), atmospheric CO_2 pressure (C_a), latitude (θ) and several other minor parameters. The model can then be solved analytically to predict that VD is positively linked to T_c and negatively linked to C_a, (Fig. 4, Supporting Information Fig. S1), consistent with other theories (Brodribb & Feild, 2010; de Boer *et al.*, 2012). A key assumption of the theory is that the appropriate community-mean VD can be achieved either through evolutionary lability or species sorting, such that trait values reflect an adaptive response to local climate rather than biogeographic history.

We test the theory's predictions and assumptions using data from modern plant communities. We measure VD on 1048 leaves of 187 nonmonocot angiosperm species at 17 sites ranging across a 2480–3370 m temperate elevation gradient and a 60–3250 m tropical elevation gradient. We first assess empirical correlations between community-mean VD and elevation. We then compare the model's predictions for growing season temperature and atmospheric CO_2 concentration to values predicted from each community's species-mean vein density.

Description

Theory

We develop a model to approximate the physiology of C_3 angiosperm species with abaxial stomata. C_3 species dominate terrestrial ecosystem productivity, comprise the largest fraction of contemporary plant diversity, as well as the paleodiversity after the late-Mesozoic angiosperm radiation (Stewart & Rothwell, 1993). In principle, the model could be expanded to include the specific anatomies and physiologies of other groups (e.g. gymnosperms, ferns, bryophytes or monocots). All model parameters are summarized in Table 1.

A key assumption is that, under 'ideal conditions', leaf water supply (E; transpiration rate; mmol m^{-2} s^{-1}) is proportional (α; dimensionless) to environmental water demand (PET; potential evapotranspiration; mmol m^{-2} s^{-1}) where:

$$E = \alpha \cdot \mathrm{PET} \qquad \text{Eqn 1}$$

Here, 'ideal conditions' means that the model will be most valid when leaves are functioning at low levels of physiological stress (e.g. open stomata and favorable leaf–stem water potentials). As a result, the venation network, which is constructed early during leaf development (Sack *et al.*, 2012), should have a structure that matches, but does not exceed, the environmental demands that the leaf is likely to experience over a typical lifespan. This hypothesis is consistent with the coordination of leaf hydraulics with environmental conditions in several species (Brodribb & Jordan, 2011; Carins Murphy *et al.*, 2012, 2014; Blonder *et al.*, 2013). Moreover, variation in leaf minor vein density matches variation in environmental water demand (Uhl & Mosbrugger, 1999; Givnish *et al.*, 2005; Sack & Frole, 2006; Brodribb & Feild, 2010; Brodribb & Jordan, 2011) at both the developmental and evolutionary timescales (but see Feild *et al.*, 2011).

Next, we assume that leaf transpiration rate, E, will be related to the leaf–stem water potential, $\Delta\Psi_{ls}$ (MPa); and the leaf hydraulic path length d_m (μm). We formally link E, $\Delta\Psi_{ls}$ and d_m

Table 1 Summary of model parameters

Symbol	Name	Units	Central value	Half-width
T_c	Growing season temperature	°C	10	5
C_a	Atmospheric carbon dioxide pressure	Pa	40	10
θ	Latitude	°	9 (tropical) 39 (temperate)	1
h	Atmospheric humidity	%	60	10
D	Vapor pressure deficit	kPa	1	0.5
g_1	Stomatal conductance coefficient	–	3	2
$\Delta\Psi_{ls}$	Leaf–stem water potential	MPa	0.10	0.05
d_y	Leaf half-thickness	μm	80	30
s	Insolation factor	–	1	0.1

The central value was used to parameterize the model. Uncertainty was explored by sampling values from a uniform distribution with center and half-width given here.

© 2014 The Authors
New Phytologist © 2014 New Phytologist Trust

using an empirical relationship reported by Brodribb *et al.* (2007):

$$E = 12\,670 \cdot \Delta\Psi_{ls} \cdot d_m^{-1.27} \quad \text{Eqn 2}$$

Further, we can write d_m, the hydraulic path length (μm), as

$$d_m \equiv \frac{\pi}{2}\left(d_{iv}^2 + d_y^2\right)^{1/2} \quad \text{Eqn 3}$$

where d_y is the leaf half-thickness (μm), representing the characteristic distance from vein to abaxial stomata, and d_{iv} is the distance between minor veins, which is empirically related to vein density (VD; mm^{-1}) as

$$d_{iv} = \frac{650}{VD} \quad \text{Eqn 4}$$

Note that this transpiration model may lose some accuracy depending on the mode of water transport but deviations are important only at very high VD values (de Boer *et al.*, 2012).

The proportionality factor α empirically relates actual evapotranspiration to potential evapotranspiration (Trabucco & Zomer, 2010). This coefficient is used in the context of agricultural crop coefficients (Allen *et al.*, 1998) and is similar to the Horton index, which is defined as the ratio of water vaporization through any means to catchment wetting at the landscape scale (Troch *et al.*, 2009). We define α as the Priestley–Taylor coefficient, the fraction of surface moisture available for evaporation (Priestley & Taylor, 1972), because it can be empirically linked to stomatal conductance (eqn 3 of Komatsu, 2005):

$$\alpha = 1.26 \cdot \left(1 - e^{-g_s/5}\right) \quad \text{Eqn 5}$$

(g_s, stomatal conductance to water vapor ($mm\ s^{-1}$)).

We assume that, across differing climates, leaves maximize carbon gain per unit water loss by regulating stomatal conductance (Cowan & Farquhar, 1977). Based on a recent optimality model (Medlyn *et al.*, 2011) we use:

$$g_s = 1.6 \cdot 10^{-3}\, RT_0 \cdot \frac{A}{C_a}\left(1 + \frac{g_1}{D^{1/2}}\right), \quad \text{Eqn 6}$$

where $10^{-3}\ RT_0$ is a unit conversion factor from $mol\ m^{-2}\ s^{-1}$ to $mm\ s^{-1}$, $R = 8.31447$ J mol^{-1} K^{-1} and $T_0 = 288.15$ K, 1.6 converts from conductance of CO_2 to that of H_2O (A, the peak photosynthetic rate (μmol m^{-2} s^{-1}); C_a, atmospheric CO_2 pressure (Pa); g_1, a constant ($kPa^{1/2}$) reflecting the marginal water cost of carbon and the CO_2 compensation point for photosynthesis; D, vapor pressure deficit (kPa)). For analytic tractability, we linearize Eqn 6 in terms of C_a by performing a first-order Taylor approximation around a central value, C_a*:

$$g_s = 1.6 \cdot 10^{-3}\ RT_0 \cdot \frac{A}{D^{1/2}} \cdot \left(g_1 + D^{1/2}\right) \cdot \left(2C_a^* - C_a\right) \quad \text{Eqn 7}$$

here choosing $C_a^* = 40$ (the modern atmospheric value).

We make a further assumption that venation networks are coupled to photosynthesis (Brodribb *et al.*, 2007). Primarily for analytic tractability, we make the linear approximation that

$$A = \eta \cdot VD. \quad \text{Eqn 8}$$

We use $\eta = 1$ ($mm\ \mu mol\ m^{-2}\ s^{-1}$) based on an approximate fit to the data of (Brodribb *et al.*, 2007).

PET is modeled using a modified version of the Hargreaves–Samani (Hargreaves & Samani, 1982) model. This version was chosen because it requires relatively few parameters:

$$\mathrm{PET} = \frac{625}{972} \cdot \frac{75}{10\,000} \cdot R_a \cdot C_t \cdot T_f \cdot \Delta T^{1/2}, \quad \text{Eqn 9}$$

where the 625/972 prefactor converts from $mm\ d^{-1}$ to $mmol\ m^{-2}\ s^{-1}$ (R_a, total incident solar radiation; C_t, a humidity factor; T_f, temperature (°F); ΔT, average temperature range). We convert T_f to a Celsius temperature (T_c; °C) as $T_f = 1.8 \cdot T_c + 32$, where again, T_c is the growing season temperature, with R_a defined as

$$R_a = s \cdot 15.392 \cdot d_r \cdot (\omega_s \cdot \sin\varphi \cdot \sin\delta + \cos\varphi \cdot \cos\delta \cdot \sin\omega_s) \quad \text{Eqn 10}$$

and where s is an insolation factor (dimensionless), and orbital parameters d_r, ω_s and δ are given as

$$\begin{aligned} d_r &= 1 + 0.033 \cdot \cos\left(\frac{2\pi J}{365}\right) \\ \omega_s &= \cos^{-1}(-\tan\varphi \cdot \tan\delta) \\ \delta &= 0.4093 \cdot \sin\left(\frac{2\pi J}{365} - 1.405\right) \\ \varphi &= \frac{\pi}{180} \cdot \theta \end{aligned} \quad \text{Eqn 11}$$

(J, day of year (dimensionless); θ, latitude (°)). The humidity factor is empirically defined (Hargreaves & Samani, 1982) as

$$C_t = \begin{cases} 0.035 \cdot (100 - h)^{1/3} & h > 54 \\ 0.125 & \text{otherwise} \end{cases} \quad \text{Eqn 12}$$

where h is the relative humidity (%). The isothermality factor ΔT can be empirically written (Hargreaves & Samani, 1982) as

$$\Delta T = 10 + 0.32 \cdot (100 - h) \quad \text{Eqn 13}$$

In order to reduce the number of free parameters in the model, we use the assumption that the model applies only during the 'ideal' conditions previously described. Under these conditions, we can further parameterize the model with $J = 180$ (midsummer), $D = 1$ and $g_1 = 3$ (typical for the species being modeled) (Medlyn *et al.*, 2011) and $\Delta\Psi_{ls} = 0.10$ (typical under low water-stress conditions across diverse species) (Sack & Holbrook, 2006).

© 2014 The Authors
New Phytologist © 2014 New Phytologist Trust

Lastly, we assume that leaf thickness is a constant. This simplifying assumption reduces the dimensionality of the model and makes it possible to use the model for paleoclimate applications. Thickness cannot be easily measured on fossil leaves. We choose $d_y = 80$ because it represents many common species and is commonly used in other paleoecological models (de Boer *et al.*, 2012). Modern insolation intensities are by definition characterized by $s = 1$. Across paleotime, the value of s may be variable, depending on orbital variation, solar output (Laskar *et al.*, 2011) and mean cloudiness.

We solve the above equations analytically to predict atmospheric carbon dioxide C_a (or T_c) based on measured values of leaf venation, VD, the growing season temperature T_c (or C_a), latitude θ and relative humidity h. While the solutions are too large to present here, they are shown in full in the Supporting Information (Eqns S1–S3 in Notes 1). We also provide a *Mathematica* notebook (Notes S2) for direct manipulation and parameterization of the model. In general, higher values of VD are predicted to yield higher values of T_c or lower values of C_a, if all other parameters are held constant. The analytic form of these equations also makes it possible to explore the consequences of variation in traits that we assumed to be constant (e.g. leaf thickness, water potential).

Field collections

We tested predictions of our model by collecting leaves from species found within 17 sites along a temperate and tropical elevation gradient (Table 2). At each site we measured latitude and longitude using a GPS unit. For tropical sites, elevation was obtained directly from satellites; for temperate sites, elevation was obtained from a digital elevation model (USGS, National Elevation Dataset).

The temperate gradient was located in the Gunnison Valley of western Colorado in the United States (39°N) and included 11 sites (each *c.* 1 m^2) ranging in elevation from *c.* 2440 to 3370 m asl. These sites span a continuum from arid montane riparian areas to alpine meadow and include both woody and herbaceous species. During the 2010 growing season we sampled the more common nonmonocot angiosperm species ($n = 6 \pm 3$ SD), taking several (9 ± 1 SD) mature undamaged leaves from individuals of each species.

The tropical gradient was located in the Savegre River drainage of western Costa Rica (9°N) and included six sites ranging in elevation from 65 to 3250 m. These sites span a continuum from tropical moist forest to tropical wet montane forest and include only woody species. For each site we set up a 0.1-ha 'Gentry transect' (Phillips & Miller, 2002), identifying every individual with dbh ≥ 2.5 cm. We then sampled at least one leaf from at least one individual of every observed species. At each site, we then chose a random subset of fifty leaves, each from a different individual for venation analysis. We took this random sampling approach because the high diversity at these tropical sites (mean richness = 68 ± 31 SD species) made a full analysis of all leaves time-prohibitive.

Vein density measurements

All leaves were pressed flat and dried at 60°C for at least 3 d. We then cleared each leaf to expose its venation using established protocols (Pérez-Harguindeguy *et al.*, 2013). We cut a 1-cm^2 section from each leaf, selecting a region of the lamina that did not include any primary veins. We immersed the leaf sample in a solution of 5% w/v sodium hydroxide : water heated to a temperature of 50°C for up to 7 d, until the leaf became transparent. We then rinsed the leaf in water and transferred it to a 2.5% w/v sodium hypochlorite : water solution for up to 5 min, until the leaf became white. We then rinsed the leaf in water and transferred it to 50% v/v ethanol : water solution for 5 min, and then to a staining solution of 0.1% w/v safranin : ethanol for 30 min. We then transferred the leaf to a destaining solution of 100% ethanol for 1 h before transferring to 50% v/v ethanol : toluene for 30 s and then to 100% toluene. We then mounted each leaf on a glass slide using the toluene-based Permount medium (Fisher Scientific, Waltham, MA, USA). We allowed slides to dry for 3 d during which the clearing process continued. Some samples were inadvertently destroyed by this chemical process. The final dataset included 225 tropical leaves and 529 temperate leaves from 187 nonmonocot angiosperm species.

We then imaged each leaf using a dissecting microscope (SZX-12; Olympus) coupled to a digital camera (T2i; Canon, Japan). Slides were back-illuminated using a light box. Images were obtained at a final resolution of 430 pixels per millimeter with a full extent of *c.* 10 mm × 7 mm. We then retained only the green channel of each image and applied a contrast-limited adaptive histogram equalization procedure to improve image quality.

We estimated vein density on each image using a stochastic line-intersection technique. The distance between veins is known to strongly correlate with the density of veins (Uhl & Mosbrugger, 1999; Brodribb *et al.*, 2007). Distance can be rapidly estimated by counting the number of veins crossed by a line of a known length (cartooned in Fig. S1). To calibrate this approach, we first used a collection of previously traced leaves from 25 morphologically diverse species (Blonder *et al.*, 2011) on which we simulated the placement of a number of randomly oriented line segments. We then compared the known vein density of the leaf to the mean distance between veins, as estimated as the total length of all line segments divided by the total number of vein intersections.

For as few as 10 random line segments (*c.* 7 cm total length) there was a very strong correlation ($r^2 = 0.89$, $P < 10^{-15}$) between vein density (VD, mm^{-1}) and distance (d, mm):

$$\mathrm{VD} = 0.629 \cdot \left(\frac{1}{d}\right) + 1.073 \qquad \text{Eqn 14}$$

We then pooled leaf-level measurements to calculate species-at-site mean vein densities and used these to then estimate site-mean vein density. We used species-at-site means because some species occurred at multiple sites, potentially obscuring trait variation due to between-site climate variation.

© 2014 The Authors
New Phytologist © 2014 New Phytologist Trust

Table 2 Summary of collections at each location (the number of leaves collected follows each species name)

Elevation (m asl)	Taxa
Tropical	
65	Annonaceae/*Oxandra venezuelana* (1), Apocynaceae/*Aspidosperma desmanthum* (3), Bignoniaceae/*Arrabidaea* sp.2 (1), Bignoniaceae/*Callichlamys latifolia* (1), Boraginaceae/*Cordia* sp.2 (1), Chrysobalanaceae/*Licania operculipetala* (1), Clusiaceae/*Calophyllum longifolium* (1), Connaraceae/*Rourea glabra* (1), Erythroxylaceae/*Erythroxylum macrophyllum* (3), Fabaceae/*Clitoria javitensis* (1), Fabaceae/*Machaerium kegelii* (1), Fabaceae/*Machaerium salvadorense* (1), Fabaceae/*Swartzia ochnacea* (1), Icacinaceae/*Discophora guianensis* (1), Lacistemataceae/*Lacistema aggregatum* (2), Lauraceae/*Nectandra umbrosa* (3), Lauraceae/*Ocotea leucoxylon* (1), Melastomataceae/*Mouriri gleasoniana* (2), Meliaceae/*Ruagea glabra* (2), Moraceae/*Trophis involucrata* (1), Myrtaceae/*Eugenia acapulcensis* (1), Myrtaceae/*Myrciaria floribunda* (1), Rubiaceae/*Faramea occidentalis* (1), Salicaceae/*Tetrathylacium johansenii* (1), Sapotaceae/*Pouteria chiricana* (3)
500	Brassicaceae/*Capparis frondosa* (1), Burseraceae/*Protium glabrum* (1), Burseraceae/*Protium* sp.1 (1), Clusiaceae/*Garcinia intermedia* (1), Clusiaceae/*Tovomita longifolia* (1), Fabaceae/*Inga coruscans* (1), Fabaceae/*Macrolobium costaricense* (1), Fabaceae/*Swartzia ochnacea* (1), Lauraceae/*Nectandra umbrosa* (1), Moraceae/*Clarisia biflora* (1), Moraceae/*Pseudolmedia glabrata* (1), Moraceae/*Sorocea hispidula* (1), Myristicaceae/*Compsoneura excelsa* (3), Myristicaceae/*Virola guatemalensis* (1), Myrtaceae/*Eugenia acapulcensis* (2), Rubiaceae/*Chione venosa* (1), Salicaceae/*Lunania mexicana* (1), Salicaceae/*Tetrathylacium johansenii* (1), Sapotaceae/*Chrysophyllum* sp.2 (1), Violaceae/*Rinorea crenata* (8), Violaceae/*Rinorea hummelii* (1), Violaceae/*Rinorea squamata* (2), Vochysiaceae/*Vochysia megalophylla* (1)
1050	Annonaceae/*Guatteria diospyroides* (1), Apocynaceae/*Lacmellea zamorae* (2), Burseraceae/*Protium* sp.3 (1), Burseraceae/*Protium* sp.4 (1), Dichapetalaceae/*Dichapetalum* sp.1 (1), Euphorbiaceae/*Croton megistocarpus* (1), Euphorbiaceae/*Hieronyma oblonga* (1), Euphorbiaceae/*Richeria dressleri* (2), Fabaceae/*Entada gigas* (1), Fabaceae/*Inga latipes* (1), Fabaceae/*Inga thibaudiana* (1), Icacinaceae/*Discophora guianensis* (1), Lauraceae/*Licaria* sp.1 (1), Lauraceae/*Ocotea meziana* (1), Lauraceae/*Ocotea praetermissa* (1), Moraceae/*Brosimum guianense* (2), Moraceae/*Pseudolmedia glabrata* (1), Moraceae/*Pseudolmedia mollis* (1), Myrsinaceae/*Ardisia dunlapiana* (2), Myrtaceae/*Myrcia* sp.2 (1), Rubiaceae/*Coussarea caroliana* (2), Rubiaceae/*Coussarea loftonii* (2), Rubiaceae/*Faramea* sp.1 (1), Rubiaceae/*Posoqueria coriacea* (1), Rubiaceae/unknown sp.1 (1), Sapindaceae/*Matayba apetala* (1), Sapotaceae/*Chrysophyllum* sp.2 (1), Sapotaceae/*Chrysophyllum* sp.3 (1), Sapotaceae/*Pouteria chiricana* (1), Verbenaceae/*Aegiphila* sp.1 (1), Vochysiaceae/*Vochysia allenii* (1)
2050	Annonaceae/*Guatteria oliviformis* (1), Aquifoliaceae/*Ilex skutchii* (1), Aquifoliaceae/*Ilex* sp.2 (1), Araliaceae/*Dendropanax querceti* (2), Araliaceae/*Oreopanax xalapensis* (6), Asteraceae/*Verbesina oerstediana* (4), Bignoniaceae/*Amphitecna sessilifolia* (1), Brunelliaceae/*Brunellia costaricensis* (2), Fagaceae/*Quercus copeyensis* (1), Fagaceae/*Quercus rapurahuensis* (1), Fagaceae/*Quercus seemannii* (2), Lauraceae/*Ocotea insularis* (5), Lauraceae/*Ocotea praetermissa* (1), Lauraceae/*Ocotea* sp.1 (1), Lauraceae/*Ocotea valeriana* (1), Magnoliaceae/*Magnolia poasana* (1), Myrsinaceae/*Ardisia* sp.3 (1), Myrsinaceae/unknown sp.2 (2), Rubiaceae/*Palicourea* sp.2 (1), Rubiaceae/*Rondeletia amoena* (1), Rubiaceae/*Rondeletia buddleioides* (2), Sabiaceae/*Meliosma vernicosa* (5)
2430	Aquifoliaceae/*Ilex* sp.2 (1), Aquifoliaceae/*Ilex* sp.3 (1), Araliaceae/*Dendropanax querceti* (1), Asteraceae/*Verbesina oerstediana* (1), Brunelliaceae/*Brunellia costaricensis* (1), Caprifoliaceae/*Viburnum stellatotomentosum* (1), Chloranthaceae/*Hedyosmum goudotianum* (2), Cornaceae/*Cornus disciflora* (2), Cunoniaceae/*Weinmannia pinnata* (2), Ericaceae/*Satyria warszewiczii* (1), Ericaceae/*Vaccinium consanguineum* (2), Fagaceae/*Quercus copeyensis* (3), Fagaceae/*Quercus rapurahuensis* (1), Fagaceae/*Quercus seemannii* (1), Juglandaceae/*Alfaroa costaricensis* (3), Lauraceae/*Nectandra cufodontisii* (1), Lauraceae/*Ocotea pittieri* (3), Magnoliaceae/*Magnolia sororum* (1), Malpighiaceae/*Bunchosia ternata* (2), Melastomataceae/*Miconia* sp.1 (1), Meliaceae/*Trichilia havanensis* (3), Myrsinaceae/*Ardisia glandulosomarginata* (3), Myrsinaceae/*Myrsine juergensenii* (3), Rubiaceae/*Palicourea salicifolia* (1), Rutaceae/*Zanthoxylum melanostictum* (1), Styracaceae/*Styrax argenteus* (1), Symplocaceae/*Symplocos retusa* (1)
3250	Araliaceae/*Oreopanax xalapensis* (1), Araliaceae/*Schefflera rodriguesiana* (2), Asteraceae/*Diplostephium costaricense* (2), Celastraceae/*Maytenus woodsonii* (2), Clethraceae/*Clethra gelida* (2), Clusiaceae/*Hypericum irazuense* (1), Cunoniaceae/*Weinmannia pinnata* (3), Ericaceae/*Comarostaphylis arbutoides* (2), Ericaceae/*Macleania rupestris* (2), Ericaceae/*Vaccinium consanguineum* (3), Escalloniaceae/*Escallonia myrtilloides* (1), Fagaceae/*Quercus costaricensis* (1), Garryaceae/*Garrya laurifolia* (3), Melastomataceae/*Miconia schnellii* (1), Melastomataceae/*Miconia talamancensis* (2), Myrsinaceae/*Myrsine dependens* (2), Rhamnaceae/*Rhamnus oreodendron* (3), Scrophulariaceae/*Buddleja nitida* (1)
Temperate	
2437	Malvaceae/*Sphaeralcea coccinea* (9), Rosaceae/*Prunus emarginata* (9), Rosaceae/*Prunus virginiana* (9), Rosaceae/*Rosa acicularis* (9), Salicaceae/*Populus angustifolia* (9)
2481	Asteraceae/*Artemisia tridentata* (9), Asteraceae/*Balsamorhiza sagittata* (9), Asteraceae/*Psilochenia occidentalis* (9), Rosaceae/*Amelanchier utahensis* (9), Scrophulariaceae/*Castilleja chromosa* (9)
2706	Asteraceae/*Chrysanthemum leucanthemum* (9), Asteraceae/*Senecio integerrimus* (9), Asteraceae/*Taraxacum officinale* (9), Brassicaceae/*Thlaspi montanum* (9), Fabaceae/*Lupinus bakeri* (9), Ranunculaceae/*Delphinium nuttalianum* (9), Rosaceae/*Geum triflorum* (9), Rosaceae/*Pentaphylloides floribunda* (9), Salicaceae/*Salix wolfii* (3), Valerianaceae/*Valeriana edulis* (9), Valerianaceae/*Valeriana occidentalis* (9)
2807	Asteraceae/*Achillea millefolia* (9), Asteraceae/*Chrysothamnus parryi* (9), Asteraceae/*Erigeron speciosus* (9), Asteraceae/*Hymenoxys hoopesii* (9), Fabaceae/*Lathyrus lanzwertii* (9), Fabaceae/*Vicia americana* (9), Geraniaceae/*Geranium viscossimum* (9), Polygonaceae/*Erigonum umbellatum* (9), Rosaceae/*Potentilla gracilis* (9), Salicaceae/*Salix* sp.1 (9), Salicaceae/*Salix* sp.2 (9), Violaceae/*Viola sororia* (9)
2873	Asteraceae/*Artemisia frigida* (9), Fabaceae/*Trifolium repens* (9), Onagraceae/*Epilobium angustifolium* (9)
2889	Berberidaceae/*Mahonia repens* (9), Polemoniaceae/*Polemonium foliosissimum* (9), Rosaceae/*Rubus idaeus* (9)
2921	Adoxaceae/*Sambucus racemosa* (9), Asteraceae/*Arnica cordifolia* (9), Orobanchaceae/*Pedicularis bracteosa* (9), Rosaceae/*Fragaria virginiana* (9)
2922	Caprifoliaceae/*Loniceria involucrata* (9), Celastraceae/*Paxistima myrsinites* (9)
2940	Apiaceae/*Osmorhiza occidentalis* (9), Geraniaceae/*Geranium richardsonii* (9), Ranunculaceae/*Thalictrum fendleri* (9), Rubiaceae/*Galium septentrional* (9), Salicaceae/*Populus tremuloides* (9)

© 2014 The Authors
New Phytologist © 2014 New Phytologist Trust

Table 2 (Continued)

Elevation (m asl)	Taxa
3162	Apiaceae/*Heracleum sphondylium* (9), Boraginaceae/*Mertensia fusiformis* (9), Crassulaceae/*Sedum rosea* (9), Onagraceae/*Epilobium angustifolium* (9)
3171	Apiaceae/*Ligusticum tenuifolium* (9), Boraginaceae/*Hydrophyllum capitatum* (9), Grossulariaceae/*Ribes montigenum* (9), Ranunculaceae/*Aquilegia coerulea* (9)
3357	Gentianaceae/*Frasera speciosa* (9), Papaveraceae/*Corydalis caseana* (9)
3368	Asteraceae/*Erigeron* sp.2 (9), Asteraceae/*Heterotheca villosa* (9), Gentianaceae/*Gentiana affinis* (9), Polygonaceae/*Rumex densiflorus* (9)

Phylogenetic analysis

We conducted a phylogenetic analysis of VD using species-mean values and a phylogeny constructed with Phylocom's 'phylomatic' tool (Webb *et al.*, 2008) using the R2010 tree with branch lengths adjusted using the default Wikstrom ages file (Wikström *et al.*, 2001). We then calculated Blomberg's K statistic (Blomberg *et al.*, 2003) using species-mean values of VD.

Model parameterization and test

The values of model parameters are listed in Table 1. Sites were assigned θ values corresponding to their GPS-measured latitude (all temperate sites within 0.2° of 38.8°N; all tropical within 0.1° of 9.4°N). Site temperature (T_c) was defined as the 1950–2000 average of mean growing season temperature. This temperature was determined from 30 arcsecond-resolution Worldclim data (BIO10 variable) (Hijmans *et al.*, 2005) using each site's latitude/longitude coordinates. Site CO_2 pressure (C_a) was inferred based on a standard elevational lapse. We used site elevation ε (meters) to parameterize the barometric formula for an isothermal atmosphere:

$$C_a = C_a^* \cdot e^{-\frac{\varepsilon g M}{R T_0}} \quad \text{Eqn 15}$$

($g = 9.80665\ \mathrm{m\ s^{-2}}$; $M = 0.0289644\ \mathrm{kg\ mol^{-1}}$; and $C_a^* = 40$ Pa). When C_a was inferred, observed values of T_c were used to parameterize the model. Conversely observed values of C_a were used when inferring T_c.

Model uncertainty analysis

We measured the impact on T_c and C_a of two classes of uncertainty in the model: sampling error in VD and systemic error in all other model parameters. We first solved the model analytically for T_c and C_a. To assess systemic error in all model parameters, we assumed that the remaining parameters (D, $\Delta\Psi_{ls}$, g_1, d_y, s) were random variables uniformly distributed with a central value and a half-width reflecting to a physiologically relevant range (Table 1). When solving for T_c, we assumed that C_a was uniformly distributed between 30 and 50 Pa; when solving for C_a, we assumed that T_c was uniformly distributed between 5 and 15°C. We also allowed latitude to vary 1° in half-width around the observed value. To assess measurement error in VD, we assumed that VD was uniformly distributed between the 25% and 75% quantile of its distribution at each site. We sampled parameter values from each distribution and calculated the resulting T_c (or C_a) value.

We obtained parameter deviations by subtracting these parameter values from their central values, and prediction deviations by subtracting the T_c (or C_a) value from the value predicted when using central values for all parameters. Next, we repeated the resampling 1000 times per analysis. We calculated the middle quartile of each predicted deviation as a combined uncertainty estimate for each site. We also directly measured sampling uncertainty by solving the model, holding all parameters constant to their central values except VD, which was allowed to vary as above. All deviations are reported as interquartile ranges of these distributions.

We also measured the relative importance of each parameter to predictions of C_a (or T_c). We repeated the sensitivity analysis with the above parameter distributions, this time assuming VD to be uniformly distributed across its global range (*c.* 1–25 $\mathrm{mm^{-1}}$; Boyce *et al.*, 2009). We then constructed a linear model for deviations in C_a (or T_c) as a function of deviations in all parameters. For each parameter, we report the effect direction as the sign of the regression coefficient; and the overall effect size as the ratio of the parameter's explained sum of squares divided by the total sum of squares in an ANOVA of the linear model (i.e. an r^2 value).

Results

Distribution of vein traits

Across sites, vein density varied by an order of magnitude both across all leaves (from 1.1 to 26.3 $\mathrm{mm^{-1}}$) and across all sites 5.9–13.2 $\mathrm{mm^{-1}}$ (Fig. 1). The full dataset is available in Notes S3 and S4. Within-site variation in VD ranged from 4.8 to 18.1 $\mathrm{mm^{-1}}$ across sites. Site mean VD was negatively correlated with elevation within each gradient (tropical, $P = 0.02$, $r^2 = 0.79$; temperate, $P = 0.006$, $r^2 = 0.59$; Fig. 2). Similar relationships were observed with growing season temperature and other environmental variables correlated with elevation. The slope and intercept of this relationship varied with gradient: when pooling for both gradients, the site mean VD–elevation relationship was no longer significant ($P = 0.67$). The response of VD to

© 2014 The Authors
New Phytologist © 2014 New Phytologist Trust

environment was potentially adaptive, with the trait showing evolutionary lability. Species-mean values of VD varied across the angiosperm tree more than expected based on a Brownian model of trait evolution (Blomberg's K = 0.38, $P = 0.001$) (Fig. 3).

Model predictions

Using site-mean VD data, the model's predictions for C_a were strongly correlated with observed values of C_a (SMA regression; $r^2 = 0.65$, $P < 10^{-4}$) (Fig. 4a). The tropical dataset had a different slope than the temperate dataset ($P = 0.005$). The model's predictions for T_c, also using site-mean VD data, were similarly correlated with observed values of T_c (SMA regression; $r^2 = 0.76$, $P < 10^{-5}$) (Fig. 4b). The tropical slope was significantly different from than the temperate slope ($P = 0.03$). We also show predictions and observations of T_c and C_a directly as functions of VD in Fig. S2.

Sensitivity analysis

We found that predictions for C_a were affected most strongly by VD (Fig. 5a). Increases in d_y or decreases in $\Delta\Psi_{ls}$ could bias C_a predictions upward but the overall magnitude of the effect was limited. For our predictions for T_c, most parameters had minor effects (Fig. 5b). Two variables were notable exceptions: decreases in d_y or increases in $\Delta\Psi_{ls}$ could make an upward bias in our T_c predictions. As a result, our analyses indicate that if either d_y or $\Delta\Psi_{ls}$ directionally varies across environmental gradients then this could modulate the strength of the climate signal in VD. Similarly, systemic biases in constant values chosen for these variables could also reduce the inferred match between veins and climate.

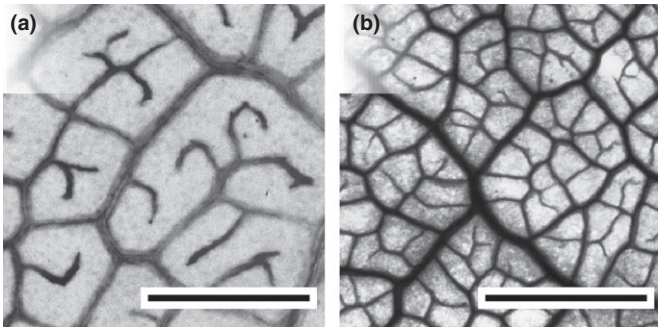

Fig. 1 Vein density is highly variable across species and sites. (a) *Escallonia myrtilloides*, from a cold tropical site (5.8 mm^{-1}); (b) *Calophyllum longifolium*, from a warm tropical site (12.4 mm^{-1}). Bars, 500 μm.

Discussion

We have developed theory that links variation in the density of the leaf venation network to species' climate niches. Specifically, the theory makes predictions for temperature and atmospheric CO_2 concentration as a function of site-mean minor vein density. We examined leaves across temperate and tropical climate gradients, and found empirical correlations between vein density and elevation. Moreover, we found that the theory predicted local climate and atmospheric composition via values of T_c and C_a across both temperate and tropical sites, albeit with some error. We also found that appropriate community-mean VD values could be obtained, either through species sorting or evolutionary trait lability. These empirical results support the key assumptions and predictions of the theory, indicating that it provides a starting point for developing more quantitative linkages between plant form and climate.

Nevertheless, the model is not a complete description of reality. While the model has high predictability, its predictions are biased in certain environments. There are four potential reasons. First, biased predictions may be due to unmeasured variation in parameters of the model. While several model parameters are difficult to directly measure, our sensitivity analysis revealed that tissue density d_y and stem water potential $\Delta\Psi_{ls}$ are the other important parameters. In this study we were not able to measure either of these parameters and so directly measure their impacts on predictions. Leaf thickness is known to vary across environmental gradients (Niinemets, 2001; Hodgson *et al.*, 2011) and could be correlated with other model parameters. Thickness may be related to VD via both functional (Noblin *et al.*, 2008; Blonder *et al.*, 2011) and developmental (Brodribb *et al.*, 2013) mechanisms, though the relationship is often unclear (Sack *et al.*, 2013). Leaf water potential, $\Delta\Psi_{ls}$, may be linked to leaf structural properties such as shrinkage (Blonder *et al.*, 2012), but shows remarkable constancy under 'ideal' conditions (Sack &

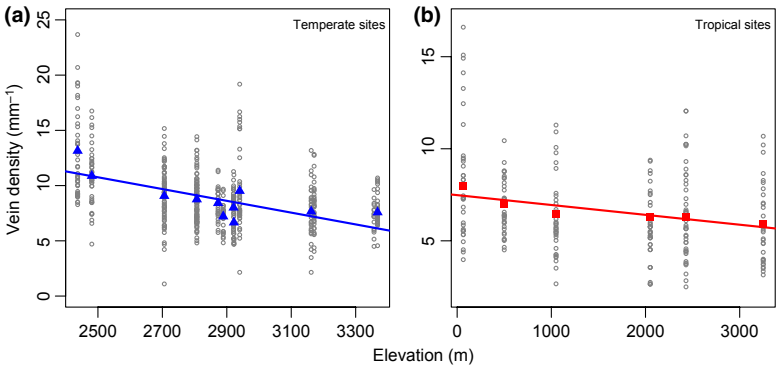

Fig. 2 Vein density is negatively correlated with elevation within regions. (a) Temperate gradient ($n = 11$ sites); (b) tropical gradient ($n = 6$ sites). Each gray symbol represents an individual leaf. Colored circles represent site means (blue triangles, temperate; red squares, tropical), and colored lines are OLS regressions for site-mean data. Note that each panel has different axis scales.

© 2014 The Authors
New Phytologist © 2014 New Phytologist Trust

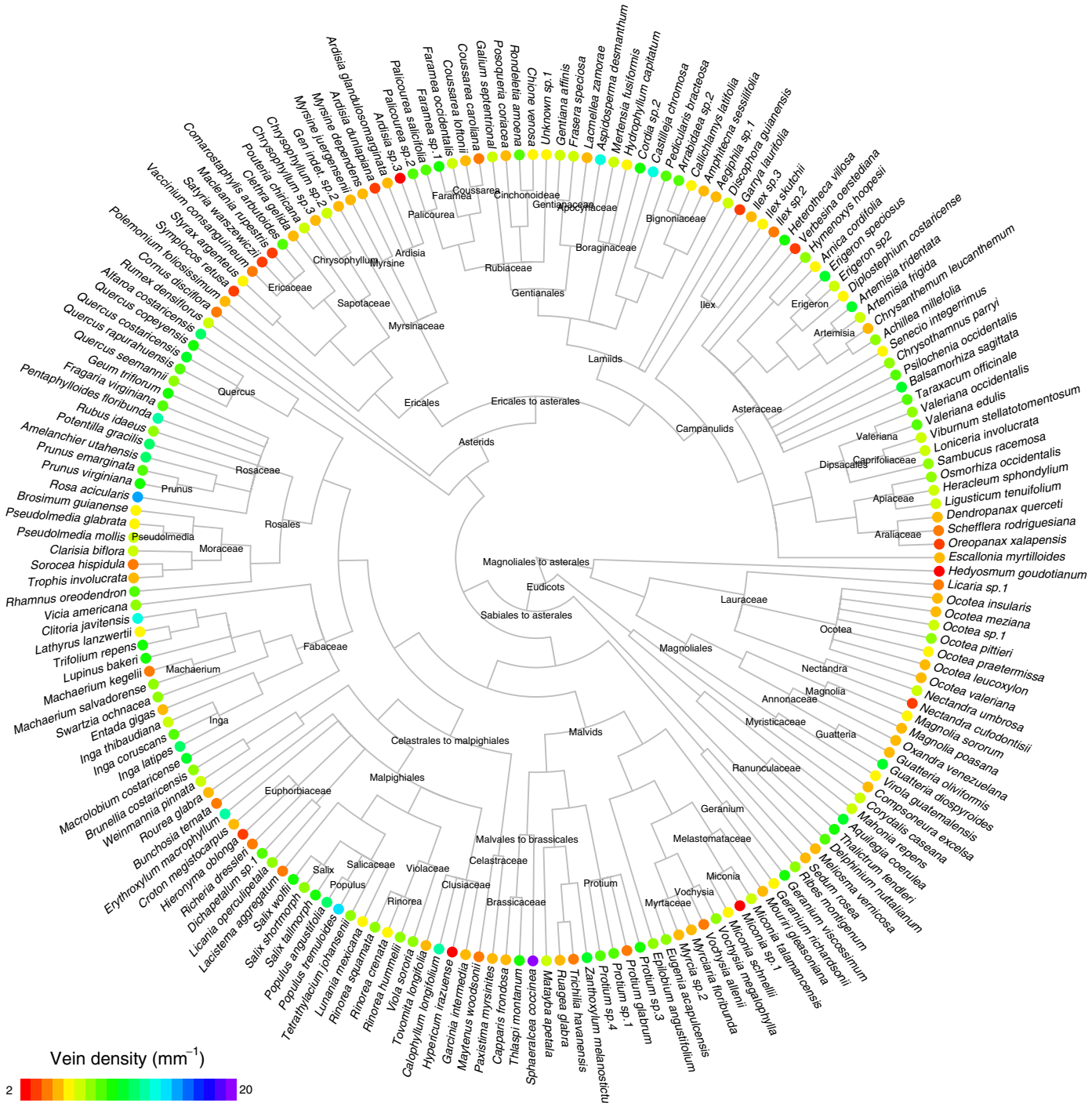

Fig. 3 Species-mean vein density is highly variable across clades. This tree includes species from both temperate and tropical sites.

Holbrook, 2006). We are unaware of any studies measuring the relationship between VD and $\Delta\Psi_{ls}$ under appropriate conditions (but see Sack & Scoffoni, 2013).

Second, observed deviations from predictions may also arise from data quality issues. While the chemical clearing method we used is a community standard (Pérez-Harguindeguy *et al.*, 2013), it may not completely clear poorly lignified leaves or those with thick palisade mesophyll or cuticular/hypodermal layers. Incomplete tissue clearing would potentially lead to underestimates of VD, lower predictions of T_c, and higher predictions of C_a than expected. Such leaves and prediction biases are found for our high-elevation tropical sites, consistent with the operation of this effect. Imaging paradermal sections of stained leaves can produce less biased measurements, though this method is far more time-consuming and less suitable for large datasets.

Third, deviations may also arise from oversimplification in the model derivation. The equations were chosen primarily for analytic tractability to operationalize the hypothesis of leaf water

© 2014 The Authors
New Phytologist © 2014 New Phytologist Trust

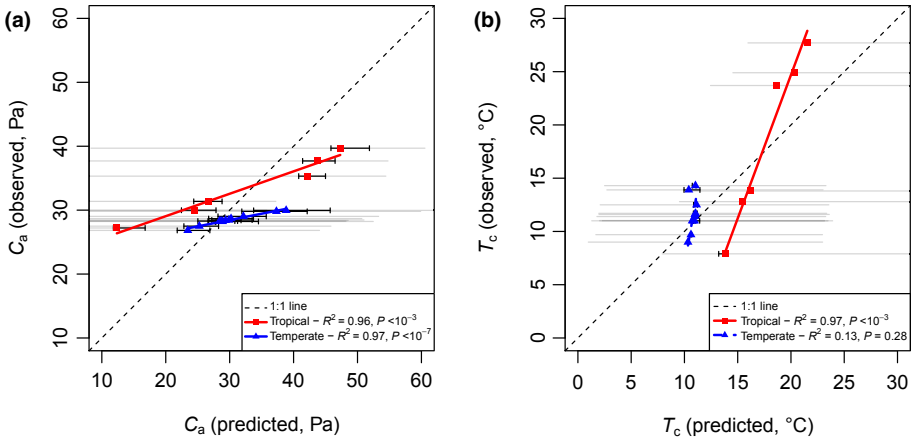

Fig. 4 Model predictions compared to observations for (a) atmospheric carbon dioxide (C_a) and (b) growing season temperature (T_c). Each colored point shows predictions based on the mean vein density for all species at each site (blue triangles, temperate; red squares, tropical). Horizontal bars show middle quartiles of uncertainty distributions: gray, for prediction uncertainty due to potential variation in all model parameters (see Table 1); black, for prediction error solely due to sampling error in vein density. Solid lines indicate standardized major axis regressions; dashed lines indicate the 1 : 1 line.

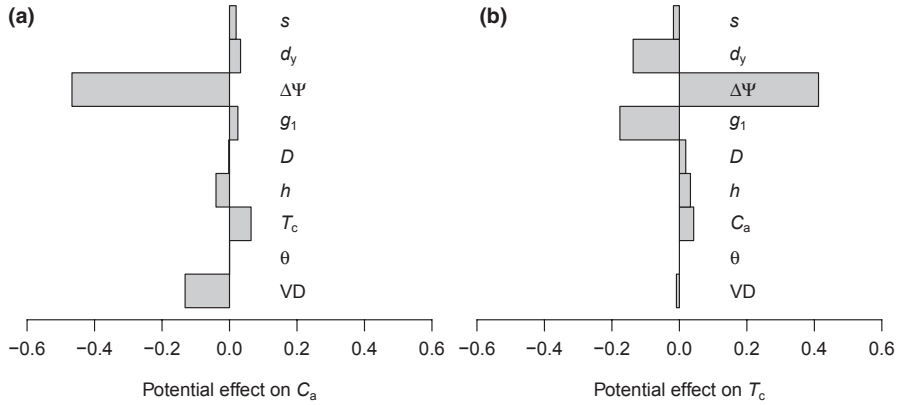

Fig. 5 Sensitivity analysis of model predictions for (a) carbon dioxide (C_a) and (b) temperature (T_c) to all parameters. The length of each gray bar indicates the importance of each variable to the model, that is, the fraction of the variance in model deviations explained by variation this parameter. Bar direction indicates the sign of the effect of each parameter on the model; that is, to the left if increases in the parameter lead to decreases in the prediction, and to the right if increases lead to increases. Parameter ranges are assumed to reflect realistic uncertainty (Table 1).

supply matching environmental demand. More precise modeling might improve predictive power. For example, the transpiration equation we used is based on a calibration for only eleven angiosperms (Brodribb *et al.*, 2007). It is also possible that the fundamental supply–demand matching assumption is not always valid. The model is likely to perform less well for species with alternative strategies for coping with evapotranspiration demand – for example, succulents, C_4/CAM species, or any species with amphistomatic or highly reflective leaves (Scoffoni *et al.*, 2011; Sack & Scoffoni, 2013). Indeed, the large range of intra-site variation in VD seen here indicates that the predicted vein–climate coupling is not achieved in all species – variation in VD or other traits may occur to match other performance requirements (e.g. sequestration of secondary compounds, mechanical strength). Similarly, woody and herbaceous species may access different water-use strategies. Such an effect could also explain the differences in slope for the temperature gradient (woody + herbaceous plants) and the tropical gradient (woody plants only). We did not have enough data to separately test the model for each growth form. Nevertheless, it is clear that VD plays an important and understudied role in determining climate niches.

Fourth, other venation network traits may also be coupled to climate in ways not explored by this model. For example, globally, species can differ extensively in the geometry of their venation network, with the same VD obtained for either highly parallel or highly reticulate patterns (Ellis *et al.*, 2009). This variation is not included in our model, as we were unable to formulate a quantitative hypothesis for the drivers of reticulation. While increasing reticulation is thought to be associated with more hydraulic redundancy (Mckown *et al.*, 2010) or damage resistance (Katifori *et al.*, 2010), there is limited available evidence for climate associations of this trait except with shady environments for monocots (Givnish *et al.*, 2005). Similarly, the geometry or density of the major veins is currently not included in our model, though these structures may also reflect variation in climate (Sack & Scoffoni, 2013). Lastly, venation network traits are known to scale with leaf area (Sack *et al.*, 2012; Blonder *et al.*, 2013), and leaf area is itself coupled to climate (Nicotra *et al.*, 2011). Understanding these potentially conflicting selection pressures is an open challenge. Future models may improve predictive accuracy by inclusion of these traits when the relevant physiological couplings are discovered.

Paleoclimate reconstruction from fossil leaf assemblages is a key application of this model. By integrating information about multiple species, the model can make robust predictions at the community scale based on first principles of leaf water balance

© 2014 The Authors
New Phytologist © 2014 New Phytologist Trust

and physiology. By contrast, other methods such as leaf margin analysis (Wolfe, 1993) and stomatal index measurements (McElwain & Chaloner, 1995; Beerling & Royer, 2002) require empirical calibration and may suffer from extrapolation problems (Jordan, 2011) or are based on a trait showing strong phylogenetic niche conservatism (Little *et al.*, 2010). Fossil leaf assemblages from applicable species with measureable venation networks are preserved from many critical periods of Earth's history (Feild *et al.*, 2011), suggesting that much may yet be inferred about past climate change.

Acknowledgements

T. Huxman, S. Saleska, J. Harte, G. Jordan, J. Sperry, K. Johnson, D. Royer and P. Wilf provided thoughtful feedback on the manuscript. B. Boyle led the tropical fieldwork. J. Bezanson, A. Henderson, N. Ioakem, D. Kahler, C. Lamanna, C. Magness, N. May, L. Parker, N. Prohaska, L. Sloat and E. Wollman assisted with data collection. B.B. was supported by a Rocky Mountain Biological Laboratory graduate research fellowship, a Geological Society of America student research grant, and a NSF pre-doctoral fellowship. B.J.E. was supported by a NSF ATB award and a NSF Macrosystems award.

References

Allen RG, Pereira LS, Raes D, Smith M. 1998. Crop evapotranspiration – guidelines for computing crop water requirements. *Irrigation and drainage paper 56*. Rome, Italy: Food and Agriculture Organization of the United Nations.

Beerling D, Royer D. 2002. Reading a CO_2 signal from fossil stomata. *New Phytologist* **153**: 387–397.

Blomberg SP, Garland T, Ives AR. 2003. Testing for phylogenetic signal in comparative data: behavioral traits are more labile. *Evolution* **57**: 717–745.

Blonder B, Buzzard V, Simova I, Sloat L, Boyle B, Lipson R, Aguilar-Beaucage B, Andrade A, Barber B, Barnes C *et al.* 2012. The leaf-area shrinkage effect can bias paleoclimate and ecology research. *American Journal of Botany* **99**: 1756–1763.

Blonder B, Violle C, Bentley LP, Enquist BJ. 2011. Venation networks and the origin of the leaf economics spectrum. *Ecology Letters* **14**: 91–100.

Blonder B, Violle C, Enquist BJ. 2013. Assessing the causes and scales of the leaf economics spectrum using venation networks in *Populus tremuloides*. *Journal of Ecology* **101**: 981–989.

Blonder B, Violle C, Patrick Bentley L, Enquist B. 2014. Inclusion of vein traits improves predictive power for the leaf economic spectrum: a response to Sack *et al.* (2013). *Journal of Experimental Botany*. doi: 10.1093/jxb/eru143.

de Boer HJ, Eppinga MB, Wassen MJ, Dekker SC. 2012. A critical transition in leaf evolution facilitated the Cretaceous angiosperm revolution. *Nature Communications* **3**: 1221.

Boyce CK, Brodribb T, Feild TS, Zwieniecki MA. 2009. Angiosperm leaf vein evolution was physiologically and environmentally transformative. *Proceedings of the Royal Society B* **276**: 1771–1776.

Boyce CK, Zwieniecki MA. 2012. Leaf fossil record suggests limited influence of atmospheric CO_2 on terrestrial productivity prior to angiosperm evolution. *Proceedings of the National Academy of Sciences, USA* **109**: 10 403–10 408.

Brodribb T, Feild TS. 2010. Leaf hydraulic evolution led a surge in leaf photosynthetic capacity during early angiosperm diversification. *Ecology Letters* **13**: 175–183.

Brodribb T, Feild T, Jordan G. 2007. Leaf maximum photosynthetic rate and venation are linked by hydraulics. *Plant Physiology* **144**: 1890.

Brodribb T, Feild TS, Sack L. 2010. Viewing leaf structure and evolution from a hydraulic perspective. *Functional Plant Biology* **37**: 488–498.

Brodribb T, Jordan G. 2011. Water supply and demand remain balanced during leaf acclimation of *Nothofagus cunninghamii* trees. *New Phytologist* **192**: 437–448.

Brodribb T, Jordan GJ, Carpenter RJ. 2013. Unified changes in cell size permit coordinated leaf evolution. *New Phytologist* **199**: 559–570.

Brodribb T, Mcadam SAM, Jordan GJ, Feild TS. 2009. Evolution of stomatal responsiveness to CO_2 and optimization of water-use efficiency among land plants. *New Phytologist* **183**: 839–847.

Carins Murphy MR, Jordan GJ, Brodribb T. 2012. Differential leaf expansion can enable hydraulic acclimation to sun and shade. *Plant, Cell & Environment* **35**: 1407–1418.

Carins Murphy MR, Jordan GJ, Brodribb T. 2014. Acclimation to humidity modifies the link between leaf size and the density of veins and stomata. *Plant, Cell & Environment* **37**: 124–131.

Carlquist S. 1959. Vegetative anatomy of *Dubautia*, *Argyroxiphium* and *Wilkesia* (Compositae). *Pacific Science* **13**: 195–210.

Cowan I, Farquhar G. 1977. Stomatal function in relation to leaf metabolism and environment. In: Jennings D, ed. *Integration of activity in the higher plant*. Cambridge, UK: Cambridge University Press, 471–505.

Díaz S, Hodgson J, Thompson K, Cabido M, Cornelissen J, Jalili A, Montserrat-Marti G, Grime J, Zarrinkamar F, Asri Y. 2004. The plant traits that drive ecosystems: evidence from three continents. *Journal of Vegetation Science* **15**: 295–304.

Dunbar-Co S, Sporck MJ, Sack L. 2009. Leaf trait diversification and design in seven rare taxa of the Hawaiian *Plantago* radiation. *International Journal of Plant Sciences* **170**: 61–75.

Ellis B, Daly D, Hickey L. 2009. *Manual of leaf architecture*. New York, NY, USA: New York Botanical Garden.

Feild TS, Brodribb T. 2013. Hydraulic tuning of vein cell microstructure in the evolution of angiosperm venation networks. *New Phytologist* **199**: 720–726.

Feild TS, Brodribb T, Iglesias A, Chatelet DS, Baresch A, Upchurch GR, Gomez B, Mohr BAR, Coiffard C, Kvacek J *et al.* 2011. Fossil evidence for Cretaceous escalation in angiosperm leaf vein evolution. *Proceedings of the National Academy of Sciences, USA* **108**: 8363–8366.

Givnish TJ, Pires JC, Graham SW, McPherson MA, Prince LM, Patterson TB, Rai HS, Roalson EH, Evans TM, Hahn WJ *et al.* 2005. Repeated evolution of net venation and fleshy fruits among monocots in shaded habitats confirms *a priori* predictions: evidence from an ndhF phylogeny. *Proceedings of the Royal Society B* **272**: 1481–1490.

Hargreaves G, Samani Z. 1982. Estimating potential evapotranspiration. *Journal of the Irrigation and Drainage Division* **108**: 223–230.

Hijmans RJ, Cameron SE, Parra JL, Jones PG, Jarvis A. 2005. Very high resolution interpolated climate surfaces for global land areas. *International Journal of Climatology* **25**: 1965–1978.

Hodgson JG, Montserrat-Martí G, Charles M, Jones G, Wilson P, Shipley B, Sharafi M, Cerabolini BEL, Cornelissen JHC, Band SR *et al.* 2011. Is leaf dry matter content a better predictor of soil fertility than specific leaf area? *Annals of Botany* **108**: 1337–1345.

Jordan G. 2011. A critical framework for the assessment of biological palaeoproxies: predicting past climate and levels of atmospheric CO_2 from fossil leaves. *New Phytologist* **192**: 29–44.

Jordan GJ, Brodribb T, Blackman CJ, Weston PH. 2013. Climate drives vein anatomy in Proteaceae. *American Journal of Botany* **100**: 1483–1493.

Katifori E, Szöllősi GJ, Magnasco MO. 2010. Damage and fluctuations induce loops in optimal transport networks. *Physical Review Letters* **104**: 048704.

Komatsu H. 2005. Forest categorization according to dry-canopy evaporation rates in the growing season: comparison of the Priestley-Taylor coefficient values from various observation sites. *Hydrological Processes* **19**: 3873–3896.

Laskar J, Fienga A, Gastineau M, Manche H. 2011. La2010: a new orbital solution for the long term motion of the Earth. *Astronomy & Astrophysics* **532**: A89. doi: 10.1051/0004-6361/201116836.

Lebedincev E. 1927. Physiologische und anatomische Besonderheiten der in trockener und feuchter Luft gezogenen Pflanzen. *Berichte der Deutschen Botanischen Gesellschaft* **45**: 83–86.

Little SA, Kembel SW, Wilf P. 2010. Paleotemperature proxies from leaf fossils reinterpreted in light of evolutionary history. *PLoS ONE* **5**: e15161.

© 2014 The Authors
New Phytologist © 2014 New Phytologist Trust

Manze U. 1967. *Die Nervaturdichte der Blätter als Hilfsmittel der Paläoklimatologie*. Köln, Germany: Geologisches Institut der Universitat zu Koln.

McElwain JC, Chaloner WG. 1995. Stomatal density and index of fossil plants track atmospheric carbon dioxide in the Palaeozoic. *Annals of Botany* **76**: 389–395.

McGill B, Enquist BJ, Weiher E, Westoby M. 2006. Rebuilding community ecology from functional traits. *Trends in Ecology & Evolution* **21**: 178–185.

Mckown AD, Cochard H, Sack L. 2010. Decoding leaf hydraulics with a spatially explicit model: principles of venation architecture and implications for its evolution. *American Naturalist* **175**: 447–460.

Medlyn BE, Duursma RA, Eamus D, Ellsworth DS, Prentice IC, Barton CVM, Crous KY, De Angelis P, Freeman M, Wingate L. 2011. Reconciling the optimal and empirical approaches to modelling stomatal conductance. *Global Change Biology* **17**: 2134–2144.

Monteith J. 1995. Accommodation between transpiring vegetation and the convective boundary-layer. *Journal of Hydrology* **166**: 251–263.

Nicotra AB, Leigh A, Boyce CK, Jones CS, Niklas KJ, Royer DL, Tsukaya H. 2011. The evolution and functional significance of leaf shape in the angiosperms. *Functional Plant Biology* **38**: 535–552.

Niinemets Ü. 2001. Global-scale climatic controls of leaf dry mass per area, density, and thickness in trees and shrubs. *Ecology* **82**: 453–469.

Noblin X, Mahadevan L, Coomaraswamy IA, Weitz DA, Holbrook NM, Zwieniecki MA. 2008. Optimal vein density in artificial and real leaves. *Proceedings of the National Academy of Sciences, USA* **105**: 9140–9144.

Pérez-Harguindeguy N, Diaz S, Garnier E, Lavorel S, Poorter H, Jaureguiberry P, Bret-Harte M, Cornwell W, Craine J, Gurvich D *et al.* 2013. New handbook for standardised measurement of plant functional traits worldwide. *Australian Journal of Botany* **61**: 167–234.

Phillips OL, Miller J. 2002. *Global patterns of plant diversity: Alwyn H. Gentry's forest transect data set*. St Louis, MO, USA: Missouri Botanical Garden Press.

Priestley CHB, Taylor RJ. 1972. On the assessment of surface heat flux and evaporation using large-scale parameters. *Monthly Weather Review* **100**: 81–92.

Royer D, Wilf P. 2006. Why do toothed leaves correlate with cold climates? Gas exchange at leaf margins provides new insights into a classic paleotemperature proxy. *International Journal of Plant Sciences* **167**: 11–18.

Royer D, Wilf P, Janesko D, Kowalski E, Dilcher D. 2005. Correlations of climate and plant ecology to leaf size and shape: potential proxies for the fossil record. *American Journal of Botany* **92**: 1141.

Sack L, Frole K. 2006. Leaf structural diversity is related to hydraulic capacity in tropical rain forest trees. *Ecology* **87**: 483–491.

Sack L, Holbrook NM. 2006. Leaf hydraulics. *Annual Review of Plant Biology* **57**: 361–381.

Sack L, Scoffoni C. 2013. Leaf venation: structure, function, development, evolution, ecology and applications in the past, present and future. *New Phytologist* **198**: 983–1000.

Sack L, Scoffoni C, John GP, Poorter H, Mason CM, Mendez-Alonzo R, Donovan LA. 2013. How do leaf veins influence the worldwide leaf economic spectrum? Review and synthesis. *Journal of Experimental Botany* **64**: 4053–4080.

Sack L, Scoffoni C, Mckown AD, Frole K, Rawls M, Havran JC, Tran H, Tran T. 2012. Developmentally based scaling of leaf venation architecture explains global ecological patterns. *Nature Communications* **3**: 837.

Scoffoni C, Rawls M, Mckown A, Cochard H, Sack L. 2011. Decline of leaf hydraulic conductance with dehydration: relationship to leaf size and venation architecture. *Plant Physiology* **156**: 832–843.

Soudzilovskaia NA, Elumeeva TG, Onipchenko VG, Shidakov II, Salpagarova FS, Khubiev AB, Tekeev DK, Cornelissen JHC. 2013. Functional traits predict relationship between plant abundance dynamic and long-term climate warming. *Proceedings of the National Academy of Sciences, USA* **110**: 18 180–18 184.

Stewart W, Rothwell G. 1993. *Paleobotany and the evolution of plants.* Cambridge, UK: Cambridge University Press.

Trabucco A, Zomer R. 2010. *Global soil water balance geospatial database: CGIAR Consortium for Spatial Information.* [WWW document] Available from the CGIAR-CSI GeoPortal at: http://www.cgiarcsi.org.

Troch PA, Martinez GF, Pauwels VRN, Durcik M, Sivapalan M, Harman C, Brooks PD, Gupta H, Huxman T. 2009. Climate and vegetation water use efficiency at catchment scales. *Hydrological Processes* **23**: 2409–2414.

Tumanow J. 1927. Ungenügende Wasserversorgung und das welken der pflanzen als mittel zur erhöhung ihrer dürreresistenz. *Planta; archiv für wissenschaftliche botanik* **3**: 391–480.

Tyree MT, Ewers FW. 1991. The hydraulic architecture of trees and other woody plants. *New Phytologist* **119**: 345–360.

Uhl D, Mosbrugger V. 1999. Leaf venation density as a climate and environmental proxy: a critical review and new data. *Palaeogeography, Palaeoclimatology, Palaeoecology* **149**: 15–26.

Webb CO, Ackerly DD, Kembel SW. 2008. Phylocom: software for the analysis of phylogenetic community structure and trait evolution. *Bioinformatics* **24**: 2098–2100.

Weiher E, van der Werf A, Thompson K, Roderick M, Garnier E, Eriksson O. 1999. Challenging Theophrastus: a common core list of plant traits for functional ecology. *Journal of Vegetation Science* **10**: 609–620.

Westoby M, Wright I. 2006. Land-plant ecology on the basis of functional traits. *Trends in Ecology & Evolution* **21**: 261–268.

Wikström N, Savolainen V, Chase MW. 2001. Evolution of the angiosperms: calibrating the family tree. *Proceedings of the Royal Society B* **268**: 2211–2220.

Wolfe J. 1993. A method of obtaining climatic parameters from leaf assemblages. *USGS Bulletin* **2040**: 1–75.

Supporting Information

Additional supporting information may be found in the online version of this article.

Fig. S1 Cartoon of vein density estimation procedure.

Fig. S2 Model predictions and observations as a function of site-mean vein density.

Notes S1 Analytic solutions for T_c and C_a (includes Eqns S1–S3).

Notes S2 Mathematica notebook implementing the above equations.

Notes S3 Trait measurements for all leaves (CSV format).

Notes S4 Site mean trait and climate value (CSV format).

Please note: Wiley Blackwell are not responsible for the content or functionality of any supporting information supplied by the authors. Any queries (other than missing material) should be directed to the *New Phytologist* Central Office.

© 2014 The Authors
New Phytologist © 2014 New Phytologist Trust